Final Draft
of the original manuscript:

Grabemann, I.; Weisse, R.:
Climate change impact on extreme wave conditions in the North Sea: An ensemble study
In: Ocean Dynamics (2008) Springer

DOI: 10.1007/s10236-008-0141-x

Ocean Dynamics manuscript No.
(will be inserted by the editor)

Climate Change Impact on Extreme Wave Conditions in the North Sea: An Ensemble Study

Iris Grabemann, Ralf Weisse

Institute for Coastal Research, GKSS Research Center, Geesthacht, Germany

Received: date / Revised version: date

Abstract. An analysis of today's mean and extreme wave conditions in the North Sea and their possible future changes due to anthropogenic climate change are presented. The sea state was simulated for the 30-year period 2071-2100 using the wave model WAM and an ensemble of wind field data sets for four climate change realizations as driving data. The wind field data sets are based on simulation outputs from two global circulation models (GCMs: HadAM3H and ECHAM4/OPYC3) for two emission scenarios (A2 and B2, Intergovernmental Panel on Climate Change, Special Report on Emission Scenarios). They were regionalized by the Swedish Meteorological and Hydrological Institute using the regional climate model RCAO. The effects of the climate realizations on the sea state statistics were assessed by analysing the differences between the patterns in the four CGM/emission scenario combinations and those in two control simulations representing reference wave climate conditions for the 30-year period 1961-1990.

The analysis of the four emission scenario/GCM combinations has shown that the future long-term 99 percentile wind speed and significant wave height increase by up to 7% and 18%, respectively, in the North Sea, except for signifgicant wave height off the English coast and to the north in the HadAM3H driven simulation. The climate change response in the ECHAM4/OPYC3 forced experiments is generally larger than in the HadAM3H driven simulations. The differences in future significant wave height between the different combinations are in the same order of magnitude as those between the control runs for the two GCMs. Nevertheless, there is agreement among the four combinations that extreme wave heights may increase in large parts in the southern and eastern North Sea by about 0.25 to 0.35 m (5-8% of present values) towards the end of the twenty first century in case of global warming. All combinations also show an increase in future frequency of severe sea state.

Correspondence to:
I. Grabemann
GKSS Research Center
Institute for Coastal Research
Max-Planck-Str. 1
D-21502 Geesthacht
Germany
e-mail: iris.grabemann@gkss.de

Key words. Ocean waves, Climate change, North Sea

1 Introduction

The North Sea in northern Europe (Fig. 1) is characterized by densely populated and highly industrialized coasts, by offshore activities, and by busy shipping routes. The human activities in the North Sea area are highly vulnerable to storms, storm surges and wind waves generated by these storms.

Large parts of the areas along the North Sea coast that are used for human activities are below or only slightly above today's mean sea level. They are protected by various coastal defences but storms with their high water levels and wave heights are a major threat.

In the past decades some significant fluctuations have been detected for the frequency and the strength of storms (e.g. WASA-Group 1998; Alexandersson et al. 2000; Weisse et al. 2005), as well as for the wave climate (e.g. Günther et al. 1998; WASA-Group 1998; Weisse and Günther 2007) in the North Sea, but no general trends were found. As a possible consequence of anthropogenic global warming, changes in the wind, wave, and storm surge climate may occur that would have significant impacts on the coasts and human activities.

Projection of future climate change include several uncertainties (e.g., model uncertainties, scenario uncertainties) that should be taken into account in climate impact research (e.g. Wang and Swail 2006). Addressing these uncertainties requires ensembles of model simulations with varying assumptions about future atmospheric composition (concentration of greenhouse gases and aerosols ,etc., due to different emissions), with different climate models, and with different initial conditions to study the effects of unforced natural variability. Nevertheless, production of ensembles is severely restricted by computational limitations.

Studies comprising larger areas, such as the North Atlantic, suggest some changes in wind conditions and storm surge water levels, as well as in wave climate in the case of anthropogenic climate change (e.g. Debernard et al. 2002;

Debernard and Roed 2008; Wang and Swail 2004; Wang et al. 2004). By now, studies comprising the smaller area of northern Europe and the North Sea with greater resolution are related to future wind conditions (Pryor et al. 2006) and to storm surge water levels (Woth 2005; Woth et al. 2006). These studies include ensembles of climate change realizations and suggest for the North Sea increases by less than 10% for strong westerly winds and by up to 0.3 m for the storm surge component of the water level towards the end of the twenty first century.

This publication deals with potential future changes in the wave climate for the North Sea using an ensemble of four climate change realizations for the years 2071-2100. Two different global general circulation models (CGMs: HadAM3H and ECHAM4/OPYC3) are incorporated for model uncertainties and two different scenarios (A2 and B2) from the Intergovernmental Panel on Climate Change (IPCC) Special Report on Emission Scenarios are taken into account to show a range of possible changes due to different emissions. The two scenarios A2 and B2 (Houghton et al. 2001; Nakicenovic and Swart 2000) are based on a heterogeneous world and focus on local and regional levels. While the "more worse" scenario A2 focuses on significant self-reliance and preservation of local identities, scenario B2 orients towards more environmental protection and social equity.

To calculate the future wave climate in the North Sea, the wave model WAM (WAMDI-Group 1988) was used in a nested version (Fig. 1). The four emission scenario/general circulation model (GCM) combinations of future wind conditions - used to drive the wave model - have been provided by the Swedish Meteorological and Hydrological Institute, with its regional coupled atmosphere-ocean model RCAO (Jones et al. 2004). This model was driven with boundary conditions obtained from the aforementioned two CGMs HadAM3H and ECHAM4/ OPYC3 for the two different emission scenarios A2 and B2 (Räisänen et al. 2003; Räisänen et al. 2004). The future changes in the wave climate were obtained by analyzing these four 30-year wave model runs for the years 2071 to 2100 with respect to 30-year "control" runs obtained from RCAO simulations with boundary conditions provided by HadAM3H and ECHAM4/OPYC3 for the reference climate in the years 1961-1990.

The resolution of the fine WAM grid is still relatively coarse for mapping the highly variable near-shore and wadden area topography of the North Sea. A rise in mean water level and future changes in today's topography were not taken into account in the wave model runs. Such changes are important in the shallow near-shore areas where the wave height is depth limited (e.g. Niemeyer and Kaiser 1999). The WAM simulations are most reliable for the deeper parts of the North Sea and, thus, the discussion is limited to the analysis of the simulations for areas with water depths greater than 10 m.

In the following, the future wave climate is displayed for the significant wave height and wave direction by a statistical analysis of mean and extreme values. As the wind is the main force, its future changes in speed and direction are also presented.

2 Methodology

2.1 Wave Model WAM

The impact of global warming on the sea state in the North Sea (Fig. 1) was investigated by numerical simulations, which were performed on the basis of simulation outputs from two global GCMs for two different climate change scenarios. The effects of the four combinations of scenarios and GCMs were assessed by analyzing the differences between the patterns in these climate realizations and those in two control runs representing reference climate conditions.

For the ocean wave simulations the wave model WAM cycle 4.5 (WAMDI-Group 1988) was used with two nested grids. The coarse grid with a spatial resolution of about 50 x 50 km covers the North Sea and parts of the northeastern North Atlantic, while the fine grid for the North Sea has a resolution of about 5.5 x 5.5 km (0.1° latitude x 0.05° longitude). For both grids, wave spectra were calculated with a directional discretization of 15° and at 28 frequencies ranging non-linearly from about 0.042 to 0.55 Hz. The latter corresponds to wave lengths between about 5 and 900 m. For the coarse grid, sea ice conditions from the GCM simulations were taken into account; for the fine grid, the model was run in shallow water mode. This set-up and model details correspond to those in Weisse and Günther (2007); for more details, see there.

The output of the wave model was used to calculate mean and extreme wave height statistics. A 45-year long wave hindcast for 1958 to 2002 has shown that the model is capable of reproducing such statistics at a reasonable degree of accuracy (Weisse and Günther 2007) .

The sea state simulations were done for two 30-year periods. Reference conditions were represented by simulations for 1961 to 1990 ("control runs"). A future wave climate in case of global warming is simulated for 2071 to 2100.

2.2 Forcing Data and Simulations

The near-surface marine wind fields at 10-m height used to force the wave model were taken from regionalizations of GCM outputs which were performed in the project PRUDENCE ("Prediction of Regional scenarios and Uncertainties for Defining European Climate change risks and Effects", funded by the European Union). Six 30-year simulations were produced for Europe using the coupled regional climate model RCAO from the Swedish Meteorological and Hydrological Institute (Jones et al. 2004; Rummukainen et al. 2001; Räisänen et al. 2003; Räisänen et al. 2004).

For these six 30-year slices driving data were taken from simulations with the GCMs ECHAM4/OPYC3 and HadAM3H. ECHAM4/OPYC3 (Roeckner et al. 1999) is a coupled atmosphere-ocean GCM, and HadAM3H is a high-resolution version of the atmospheric component of the Hadley Centre coupled atmosphere-ocean GCM HadCM3 (Gordon et al. 2000). For each of the two driving GCMs, three 30-year runs were undertaken with RCAO: a control run for 1961 to 1990 and two scenario runs for 2071 to 2100. The scenario runs were based on the two different IPCC emission scenarios A2 and B2 (Nakicenovic and Swart 2000). These simulations display

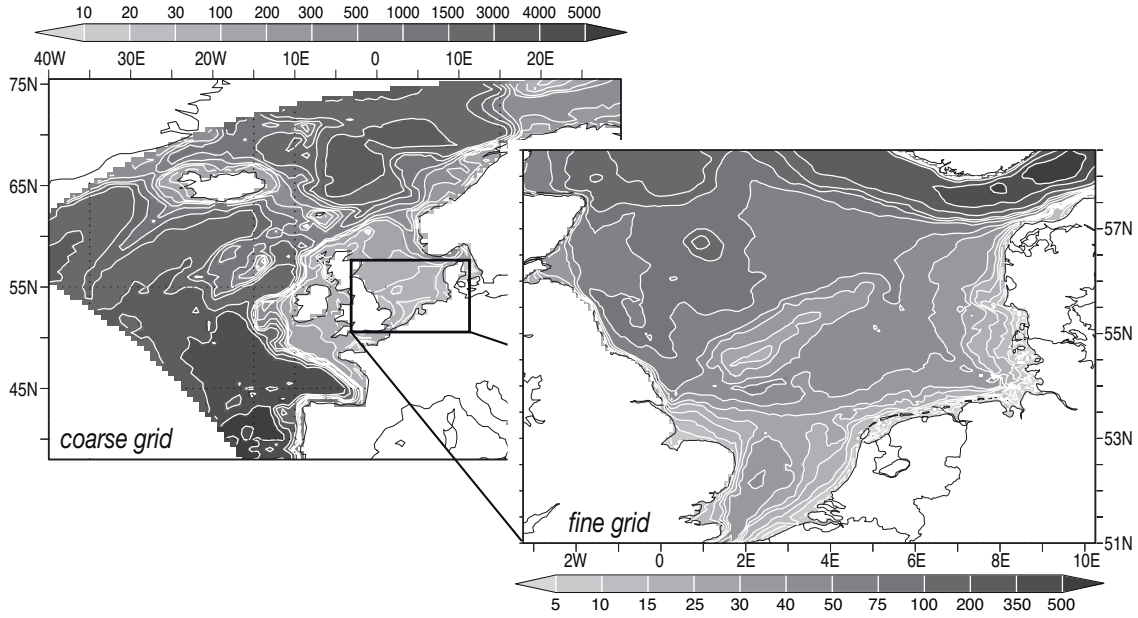

Fig. 1. Model domains used for the experiments with the wave model WAM. Left: Coarse grid covering the North Sea and parts of the Northeast North Atlantic. Right: Fine grid for the North Sea nested within the coarse grid. In both plots, grey shading indicates the water depth in meters

four realizations of possible climate change in Europe and two "control climates".

A detailed description of the RCAO simulations and a link to their forcing data sets, as well as a comprehensive analysis of the outcome of the different emission simulations, is given in Räisänen et al. (2004). The skill of the HadAM3H-driven RCAO and ECHAM4/OPYC3-driven RCAO control simulations to represent the features of the observed European climate is presented in Räisänen et al. (2003).

The near-surface marine wind fields from the six combinations of RCAO outputs are used to force the WAM simulations. They are bi-linearly interpolated to match the WAM model grids. Furthermore, sea state input data at the lateral boundaries of the fine grid are derived from the coarse grid, which covers the regions in which swell that may propagate into the North Sea may be generated.

In the following, the six different wave simulations with the model WAM and their results will be referred to as indicated in Fig. 2.

For the fine WAM grid for each of the six simulations, two-dimensional wave spectra have been stored every 3 h. Integrated wave parameters, such as significant wave height, mean wave direction, and different wave periods were extracted every hour.

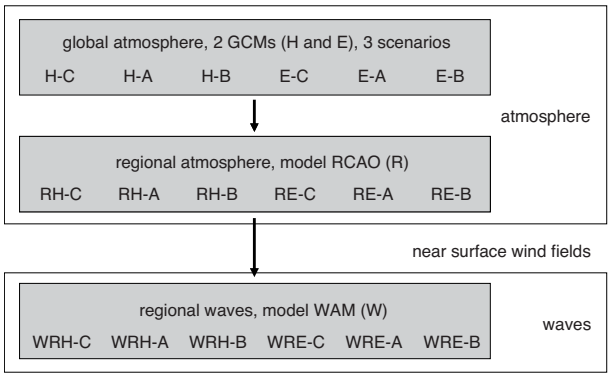

Fig. 2. Layout of the forcing and output data sets: combinations of control (C) and emission scenarios (A refers to A2; B refers to B2) and GCMs (H denotes HadAM3H; E denotes ECHAM4/OPYC3) used as driving data for the regional climate model (R, RCAO), and six WAM (W) output data sets named with respect to the six driving data sets derived from the RCAO model

2.3 Statistical Analysis

In the following, we limit ourselves to the discussion of significant wave height and direction, wind speed and direction, and number, duration and intensity of extreme events. Wind fields were included in the analysis as they represent the primary variable that determines wave behavior.

For each of the six 30-year-long model runs, the 50 and 99 percentiles ($long-term\ percentiles$) of wind speed and significant wave height were calculated. Changes in the 99 percentile are considered to be a relatively robust measure for changes in the statistics of extreme events. These long-term percentiles X^i_{ms} were calculated for every grid point i in the data set. $m = WRH, WRE$ denotes the different model combinations and $s = A, B, C$ gives the different scenarios (A and B, emission scenarios A2 and B2; C, control scenario).

Respective data from both control runs were compared to respective data from a 45-year long hindcast (Weisse and Günther 2007) to evaluate to which extent the control runs represent today's climate.

Climate signals, i.e. changes due to global climate change, were determined by analyzing the differences between the four scenario runs (the GCM/emission scenario combinations)

and the two control simulations. Thus, the climate change signal Δ^i_{ms} is defined as the difference between the value X^i_{ms} in the climate change simulation $s = A, B$ and the value from the corresponding control simulation X^i_{mC}:

$$\Delta^i_{ms} = X^i_{ms} - X^i_{mC} \quad (1)$$

Since severe wave conditions have the largest implications for many sectors, such as coastal protection, offshore constructions or shipping, this analysis is limited to extreme conditions. For a further, more detailed analysis of the climate signals in wind and wave conditions three areas with an extent of 1.5^o x 1^o near different coasts of the North Sea were selected ((1) 6.9-8.4°E, 54-55°N; (2) 0.0-1.5°E, 54.5-55.5°N; (3) 6.5-8.0°E, 56.7-57.7°N; see also the map inserted in Fig. 8).

For these areas, at first, area averaged time series of wind speed, wind direction, significant wave height and wave direction have been determined. Exceedance events (in the following referred to as $extreme\ events$) are defined in the following way. From the area-averaged time series, long-term 99 percentiles for each of the control simulations have been calculated. Subsequently, these values have been used as a threshold to derive the frequency, duration and intensity of extreme events (Fig. 3.

- The frequency N_{ms} of extreme events represents the number of exceedances of the threshold value X_{mC}.
- The mean duration D_{ms} of these events is given by the time for which the significant wave height or the wind speed remain above the respective X_{mC} divided by the number of events N_{ms} within the 30-year time slices.
- The mean intensity I_{ms} of these events is given by the intensity of all individual events within the 30-year time slices divided by N_{ms}, and the intensity of an event is defined as the difference between the threshold value X_{mC} and the maximum significant wave height or wind speed that occurred during the event.

In addition, we considered changes in the directions from which the highest 1% of all hourly values for wind and waves are coming from. The area averaged wind and wave directions were divided into 30° segments from 15°-45° to 345°-15° and the frequency with which extreme events for wind/waves coming from a particular sector was counted. Changes in the frequency distributions between control and scenario runs display if and how the dominant event wind and wave directions could change in a specific area.

The IPCC emission scenarios A2 and B2 are both plausible and consistent future projections and the formulations of both global circulation models are state-of-the-art. Nevertheless, there are uncertainties in future development of society, as well as uncertainties in the formulation of the global climate models which result in different climate change signals for the different emission/GCM combinations.

As each realization of climate change signals Δ^i_{ms} remains equally likely, we may obtain the expected value of the climate change signal from the overall ensemble mean

$$\overline{\Delta^i} = \frac{1}{MS} \sum_{m,s=1}^{M,S} \Delta^i_{ms} \quad (2)$$

by averaging over all four scenario and model realizations (M=2 GCMs and S=2 scenarios). This averaging was again performed for each grid point i. Note that hereafter the index i is dropped for convinience.

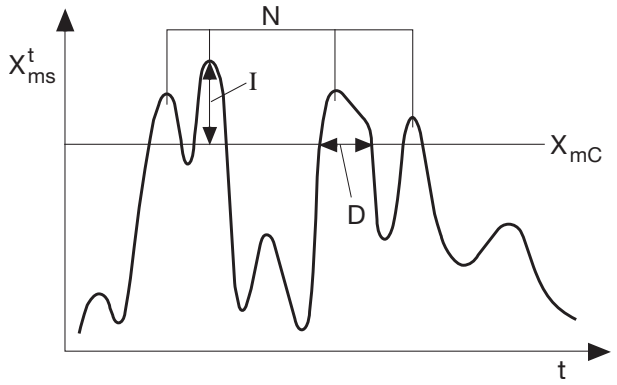

Fig. 3. Definition of parameters that characterize area averaged extreme wind and wave statistics. x^t_{ms} gives the area averaged time series of wind speed or significant wave height; X_{mC} denotes the long-term mean 99 percentile of the area averaged wave height or wind speed for the control simulations with $m = WRH, WRE$; N denotes the number of exceedance ($extreme$) events in the 30-year time slices; and D and I denote the area averaged mean duration and intensity, respectively, of each event

While the ensemble size available to us remains rather limited to make any definite statements we have anyhow made an attempt to quantify these uncertainties to get at least an impression on the magnitude of the different terms. The uncertainties in the climate change signals introduced by different model representations can be defined by

$$\Delta_{WRE,WRH} = \overline{\Delta_{WRE,s}}^s - \overline{\Delta_{WRH,s}}^s \quad (3)$$

where $\overline{(\ldots)}^s$ represents averaging over the scenarios A2 and B2 for each grid point. Similarly, the uncertainties introduced by different scenarios can be defined by

$$\Delta_{A,B} = \overline{\Delta_{m,A}}^m - \overline{\Delta_{m,B}}^m \quad (4)$$

where $\overline{(\ldots)}^m$ represents averaging over WRH and WRE.

3 Results

3.1 Validation of the Control Climate Simulations

In the following, we assess to which extent the control climate simulations represent present-day conditions. For comparison, we use multidecadal high-resolution numerical reconstructions of both, the atmosphere (Feser et al. 2001) and the North Sea wave climate (Weisse and Günther 2007). Both reconstructions cover the period 1958-2002, and it has been demonstrated that they provide a realistic description of the observed mean and extreme wind (Weisse et al. 2005; Weisse and Feser 2003) and wave (Weisse and Günther 2007) statistics. While the atmospheric reconstruction covers the entire North Sea and parts of the northeastern North Atlantic, the high-resolution wave hindcast is limited to the North Sea south of 56°N. The following comparison is therefore limited to the southern North Sea.

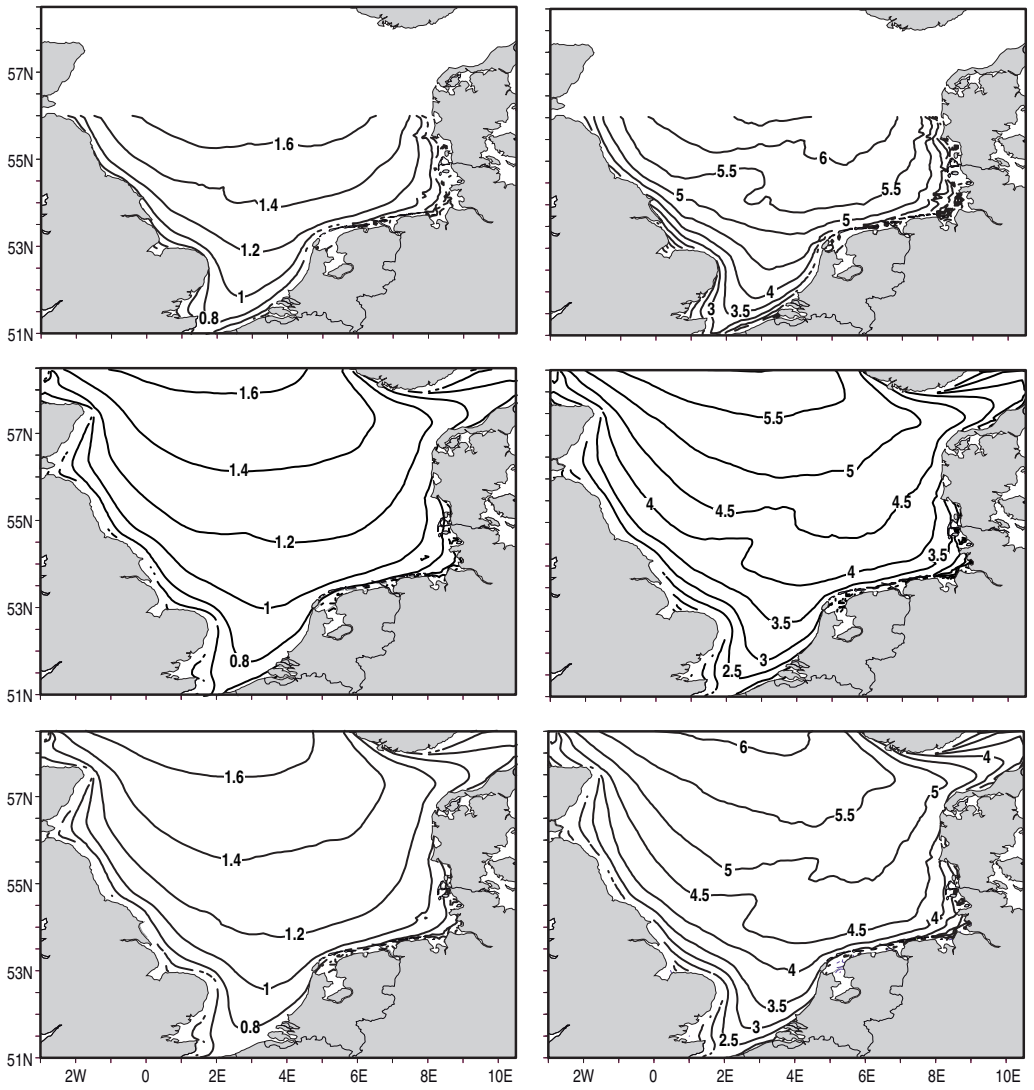

Fig. 4. Long-term 50 (left) and 99 percentile (right) significant wave height in meters obtained from the 1958-2002 multidecadal hindcast (top), the WRH control simulation (middle), and the WRE control simulation (bottom)

Figure 4 illustrates the wave climate obtained from both, the hindcast reconstruction and the two control simulations. It can be inferred that the reconstructed 1958-2002 long-term 50 percentile wave height in the southern North Sea ranges between about 1.0 and 1.6 m. The corresponding values from the control climate simulations are somewhat lower (1.0-1.4 m) while the spatial pattern is reproduced well. A similar conclusion holds for the extremes. The observed spatial pattern of the long-term 99 percentile significant wave height is well reproduced in both control simulations, while their amplitudes differ. In the reconstruction, the long-term 99 percentile wave heights vary between about 5.0 and 6.5 m, while they are only 3.5 to 5.5 m in the climate control simulations.

For wind speed, the figure is rather similar (not shown). From the 1958-2002 reconstruction, long-term 50 percentile wind speeds of about 7.5 to 8.0 m s^{-1} are obtained for the southern North Sea, while they reach only about 7.0 m s^{-1} in both climate control simulations. For the long-term 99 percentile wind speed, hindcast values for the southern North Sea vary between about 17-19 m s^{-1}, while they are only about 16-17 m s^{-1} in the control runs. Again, the spatial distributions agree well among reconstructions and control simulations.

Differences between the two control simulations are about 3% for the long-term 50 percentile of wind speed and less than 10% (smaller than 0.1 m for the entire North Sea) for the long-term 50 percentile of significant wave height (not shown). Differences in extremes are somewhat larger and may reach 1.0 m s^{-1} (about 6%) for wind speed and more than 0.45 m (about 9%) for significant wave height (Figure 5). The spatial pattern of the differences is rather similar for wind speed and wave height, with largest differences occurring in the southern North Sea just off the East and West Frisian coast.

Summarizing, it can be concluded that both climate control simulations slightly to moderately underestimate reconstructed mean conditions for both wind speed and significant wave height. The underestimation is up to 10% for wind speed and between about 10% and 15% for wave heights. Differences in extreme conditions, here represented by the

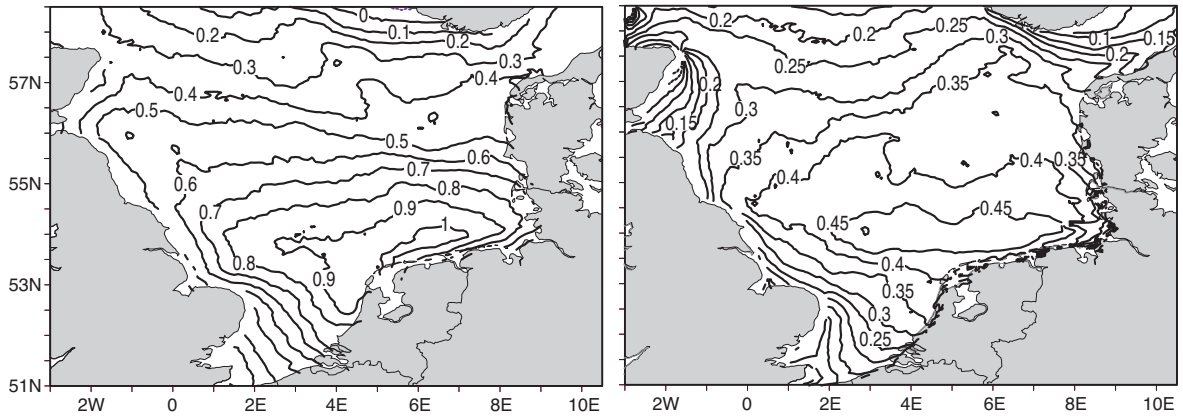

Fig. 5. Differences of long-term 99 percentile wind speed in meters per second (left) and significant wave height in meters (right) between the two climate control simulations (WRE-C minus WRH-C)

long-term 99 percentile, are considerably larger. They may reach up to 20% for some regions in the northern North Sea. While wind speed and wave height are generally too low in the control simulations, their spatial distribution shows good agreement with the observed conditions. For fully developed seas, significant wave height H_s is proportional to the square of the wind speed at 10-m height u_{10}. Roughly, it scales with $H_s[m] = 2.45(\frac{u_{10}[m/s]}{10})^2$. Considering typical climate change signals for near-surface marine wind speeds in the order of 0.5-1.0 m s^{-1}, the non-linear effects on changes in significant wave height that may arise from the underestimation of the long-term 99 percentile wind speeds are small. They are somewhat more essential for the highest 99 percentile wind speeds obtained in the northern North Sea. However, the differences become substantial only when fully developed conditions, that is unlimited fetch and duration of about 72 h or so are reached for very high wind speeds. As this is seldom the case, it is therefore suggested that, despite the deficiencies in reproducing the magnitude of the reconstructed statistics, differences between climate change and control climate simulations may be adequate to study the response of the sea state in the North Sea to changing greenhouse gas concentrations.

3.2 Climate Change Signals

In this section, we elaborate on common features and differences in the climate change signals obtained from the described experiments. Figures are mostly limited to changes in extreme (long-term 99 percentile) conditions, while changes in mean conditions are discussed without additional figures. The 99 percentile has been chosen to represent extreme conditions as its observed long-term average over the North Sea (about 17-19 m s^{-1}) corresponds with about the threshold above which conditions are said to be stormy (17.2 m s^{-1}, Beaufort scale 8).

Figure 6 shows the climate change signals (see Eq. 1) for long-term 99 percentile wind speed. For all simulations an increase for the entire North Sea is obtained. The maximum increase varies between about 0.55 m s^{-1} in the WRH-B simulation and about 1.2 m s^{-1} in the WRE-A run. In the WRH simulations, the strongest increase is found south of about 55°N, while in the WRE runs, the maximum occurs basically north of 55°N with largest values off the Danish coast. Depending on the area, the increase corresponds to about 3-7% of the long-term 99 percentile of the control simulations. If we compare the A2 with the B2 simulations, the climate change patterns are rather similar for a given model, while there is no systematic decrease in the climate change response of the B2 relative to the A2 simulations (see also section 3.4).

For long-term 50 percentile wind speed the climate change signal shows a dipole pattern in all simulations. Positive changes are found for the Skagerrak and the NE part of the North Sea. The location of the negative center of the dipole varies among the simulations. For the WRH experiments, maximum negative changes are found off the UK coast, while they are located more towards the English Channel in the WRE experiments. The magnitude of the climate change signal in long-term 50 percentile wind speed is in the order of 3-6%.

For significant wave height, a similar analysis was performed (Fig. 7). Contrary to the results for wind speed, there are larger differences among the different climate change simulations. The WRH-A simulation shows an increase in long-term 99 percentile wave height over much of the North Sea that is strongest in the southern and southeastern parts (up to 15 cm or 2-5%). For the northern parts and off the UK coast, decreases in extreme wave height conditions were found. From the WRH-B experiment, a rather similar pattern can be obtained, however, the increase in the southern North Sea is even stronger compared to the WRH-A run, and the areas with decreased extreme wave conditions have mostly disappeared. For the WRE simulations, an increase in the long-term 99 percentile wave height was found almost everywhere in the model domain, and the areas of maximum increase are located near the Skagerrak and the NE part of the North sea for both emission scenarios. The climate change response in the WRE experiments is generally much larger than in the WRH experiments (even for areas where the WRH simulations have their maximum response) and amounts up to 10-18% of the long-term 99 percentile wave height of the control simulations.

For the long-term 50 percentile wave height, a decrease in the order of about 1-7% is expected in both WRH simulations with smaller values generally occurring in the B2 run. The

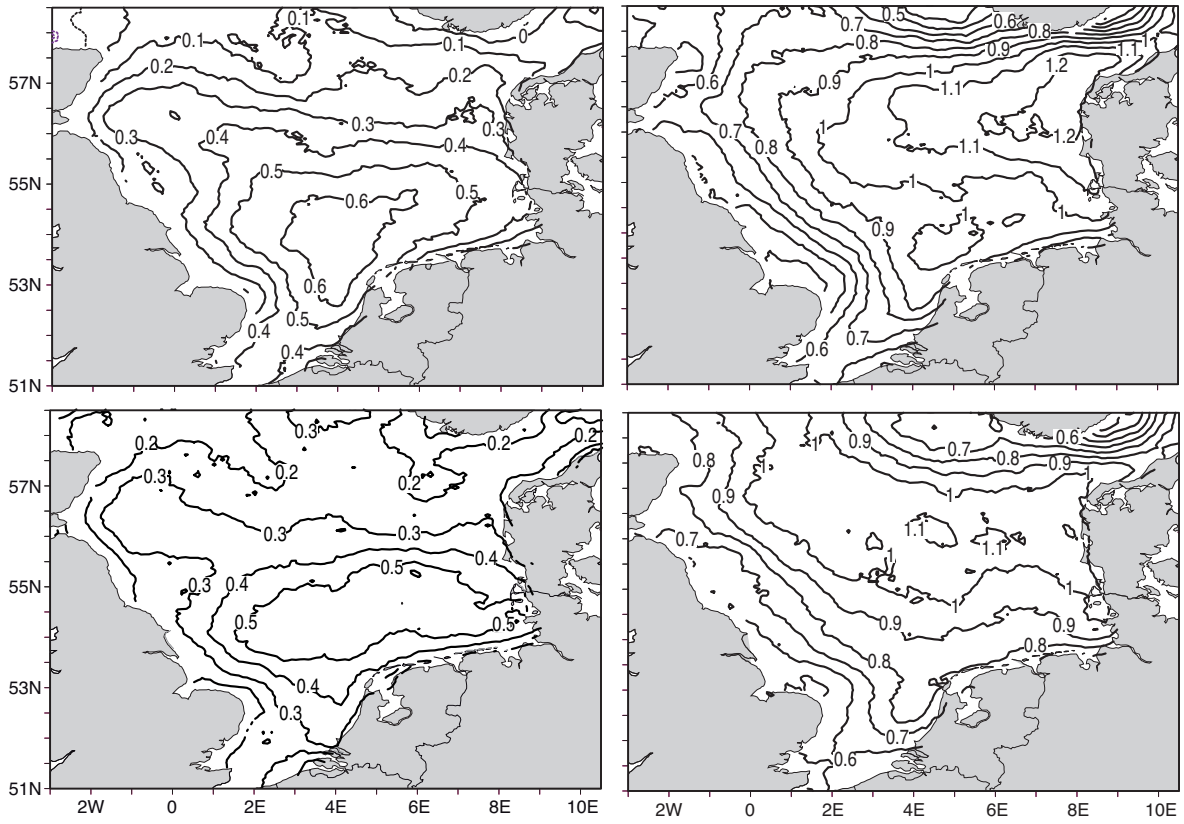

Fig. 6. Climate Change signals Δ_{ms} for long-term 99 percentile wind speed in meters per second for WRH-A (upper left), WRH-B (lower left), WRE-A (upper right), and WRE-B (lower right)

WRE experiments show a dipole pattern with decreases of about 2% in the southwestern and increases of up to 7% in the northeastern parts of the North Sea. Again, the signal in the A2 run is stronger than that in the B2 run.

In all four climate realizations, extreme significant wave heights and extreme wind speeds increase in most parts of the North Sea. Exceptions are the WRH simulations where changes in extreme significant wave height are negative in the northern and western parts of the North Sea. In the following, these changes will be analysed in more detail for three selected areas (see Fig. 8).

In all three areas and for all four climate realizations, the 99 percentile of the wind speed (Table 1) increases by about 4% to 7% (WRE realizations) and 2% to 3% (WRH realisations). The frequency of these wind events increases by 55% to 85% (highest increase in area 3, WRE) and only 10% to 20% (highest increase in area 2, WRH). Also, the duration and intensity of these extreme events increase up to 20%. Again, the changes are more pronounced in the WRE simulations. Considering the two scenarios A2 and B2, there appear to be no systematic differences. For the 99 percentile wind speed, generally, the A2 values are higher than the B2 values, but for frequency, duration, and intensity, maximum changes differ between the areas and the scenarios.

With the exception of WRH-A in area 2, the long-term 99 percentiles of the significant wave height also increase in all three areas and climate realizations. The values range from 1% to 2% for area 2 in the WRH simulations to more than 14% for area 3 in the WRE simulations (Table 2). As for wind speed, the increase in the frequency of events with extreme wave heights is higher for the WRE simulations (42% to 105% for area 3) than for the WRH simulations (4% to 12%). For the areas 1 and 3, the changes for duration and intensity of events are up to 15% and positive, except for WRH-B. For area 2, duration and intensity generally decrease up to 13% (except intensity for WRE-B). There is no clear signal that either scenario A2 or scenario B2 gives the stronger changes. In the WRE simulations, the strongest signal is the increase in the frequency of events, whereas in the WRH simulations, all changes (increase or decrease) are in the same order of magnitude.

Changes in wind (not shown) and wave direction (Fig. 8) have also been analyzed, as the fetch is as important as duration and intensity of wind events for the formation of extreme waves. For the control climate, the wind and waves during extreme events mainly come from west to northwest in areas 1 and 3 and from northwest to north in area 2. In the control simulations for area 1, 84% (WRE) and 78% (WRH) of the waves come from 255°-315°. For area 3, the respective percentages are 77 and 75. For area 2, the main total wave direction is 315°-15° (70% for the WRE and 64% for the WRH control simulation).

Generally, for all models and scenarios there is a tendency for a shift of the frequency distributions to the left. That means, in the scenario runs, the highest waves generally approach from more westerly directions in area 1, from

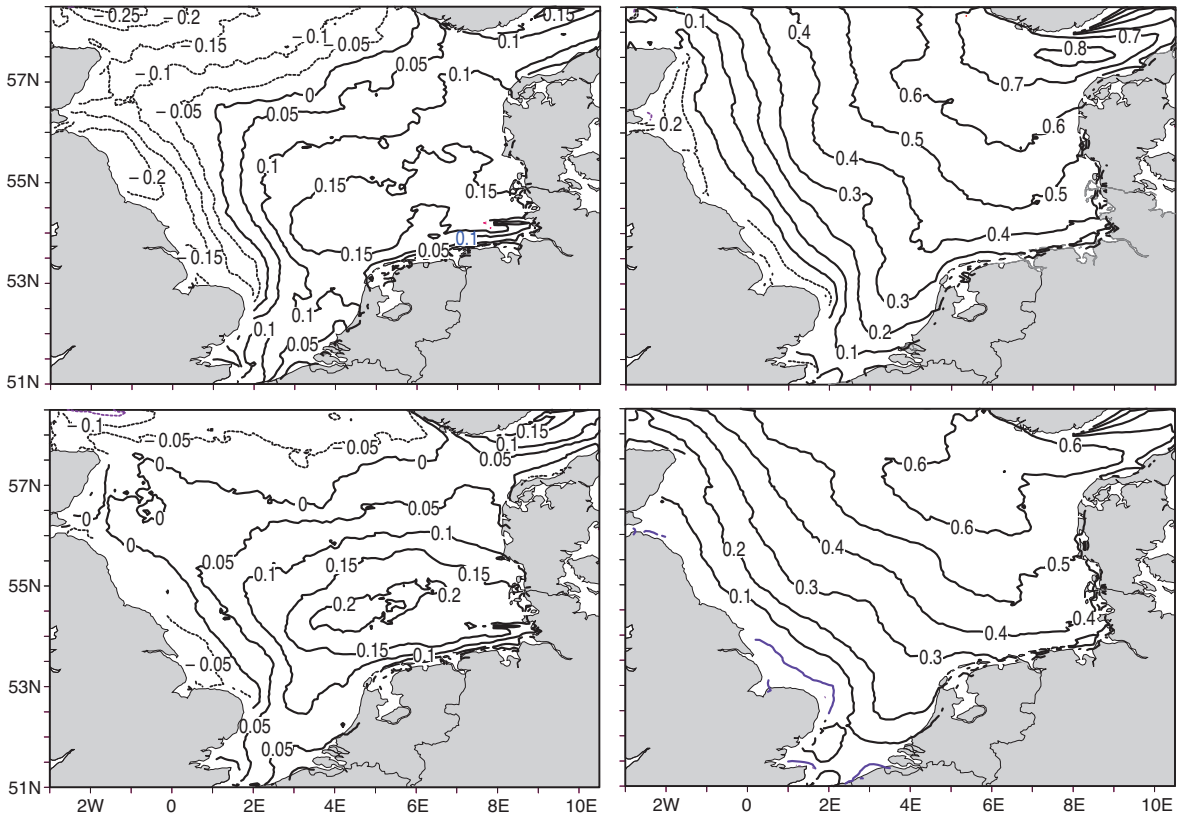

Fig. 7. Climate Change signals Δ_{ms} for long-term 99 percentile significant wave height in meters for WRH-A (upper left), WRH-B (lower left), WRE-A (upper right), and WRE-B (lower right)

Table 1. Wind speed: area averaged long-term 99 percentile (X_{ms}) in meters per second, frequency of events (N_{ms}) above the threshold value X_{ms}, mean event duration (D_{ms}) in hours, and mean event intensity (I_{ms}) in meters per second for the three selected areas and the six model/scenario combinations

	area 1				area 2				area 3			
	X_{ms}	N_{ms}	D_{ms}	I_{ms}	X_{ms}	N_{ms}	D_{ms}	I_{ms}	X_{ms}	N_{ms}	D_{ms}	I_{ms}
WRE-C	16.2	253	10.2	1.5	17.1	293	8.8	1.4	16.6	259	10.0	1.5
WRE-A	17.3	456	11.2	1.7	17.9	454	9.6	1.7	17.8	480	11.3	1.7
WRE-B	17.2	407	11.6	1.7	17.8	468	9.7	1.6	17.6	430	11.0	1.8
WRH-C	15.4	258	10.0	1.3	16.4	292	8.9	1.5	16.2	256	10.1	1.4
WRH-A	15.9	305	11.5	1.6	16.8	358	9.4	1.6	16.4	282	10.7	1.5
WRH-B	15.9	306	11.8	1.5	16.8	347	9.5	1.5	16.5	299	10.3	1.4

Table 2. Significant wave height: area averaged long-term 99 percentile (X_{ms}) in meters, frequency of events (N_{ms}) above the threshold value X_{ms}, mean event duration (D_{ms}) in hours, and mean event intensity (I_{ms}) in meters for the three selected areas and the six model/scenario combinations

	area 1				area 2				area 3			
	X_{ms}	N_{ms}	D_{ms}	I_{ms}	X_{ms}	N_{ms}	D_{ms}	I_{ms}	X_{ms}	N_{ms}	D_{ms}	I_{ms}
WRE-C	4.15	183	14.2	0.72	4.53	168	15.4	0.86	5.09	179	14.5	0.97
WRE-A	4.61	341	14.6	0.77	4.73	250	13.3	0.85	5.83	367	15.1	1.05
WRE-B	4.59	311	15.6	0.80	4.82	239	15.0	0.94	5.70	331	15.1	1.06
WRH-C	3.77	181	14.3	0.65	4.11	185	14.0	0.73	4.70	183	14.2	0.82
WRH-A	3.92	202	15.8	0.75	4.10	198	12.9	0.71	4.90	190	15.4	0.90
WRH-B	3.93	201	16.0	0.74	4.18	208	14.0	0.71	4.82	197	13.7	0.82

more northwesterly and southerly directions in area 2, and from more westerly to southwesterly directions in area 3. For the wind direction, the frequency distribution over the various sectors differs somewhat from that for the mean wave direction, while changes are broadly consistent.

In all three areas and for all four climate realizations, the increase in the frequency of severe winds seems to be a main reason for the increase in extreme wave heights. For the WRH simulations, the changes in duration and intensity may play an equally important role as the changes in frequency. The changes in wind and wave directions, which tend to more westerly sectors, may be less important as they do not significantly change the fetch.

3.3 Ensemble Mean Climate Change Signals

While there remain differences between the climate change signals from different models and different scenarios, we are not able to state which model is more reliable or which scenario is more likely to be realized. Both underlying global models (ECHAM4/OPYC3 and HadAM3H) have proven their skill in different applications, and both can be considered as state-of-the-art. The driving emission scenarios basically reflect assumptions on future socioeconomic developments. They are both consistent and plausible, but there is no consolidated forecast on how society may react in the near future. Each realization of climate change signals Δ_{ms} thus remains equally likely, and the expected value of the climate change signal from the overall ensemble mean is presented in Fig. 9 for the wind speed and for the significant wave height. In addition, it is shown for which areas, independent of model and scenario choice, the climate change signal has at least the same sign in all experiments.

For long-term 50 percentile wind speed an increase of up to 0.25 m s^{-1} (3-4%) in the Skagerrak and the northeastern North Sea, as well as a decrease of up to 0.1 m s^{-1} (1-2%) off the UK coast is obtained. Only for the Skagerrak and parts of the northeastern North Sea, the German Bight, and a very small area along the UK coast do climate change signals from all simulations obey the same sign and signals may be considered somewhat robust. For extreme wind speed (represented by the long-term 99 percentile), results are more clear. All scenarios and all model realizations indicate higher extreme wind speeds for the entire North Sea area. The ensemble mean varies between about 0.5 and 0.75 m s^{-1}, corresponding to an increase of about 3-5%.

For long-term 50 percentile significant wave height, the spatial pattern rather closely resamples that of the long-term 50 percentile wind speed with negative changes off the UK coast and positive changes in the eastern part of the North Sea. However, only for a small strip along the UK coast, the climate change signal has the same sign for all scenarios and all model realizations. Here, decreases of long-term 50 percentile significant wave height in the order of 2-5 cm may be expected. For extreme wave heights, an increase for almost the entire North Sea is obtained. For large parts, this increase is about 0.25 to 0.35 m, corresponding to about 5-8%. For large parts especially in the southern and eastern North Sea, the increase represents a robust feature as climate change signals from all experiments here have the same sign.

3.4 Uncertainties in Climate Change Signals

The analysis of climate change signals obtained from different climate model/emission scenario combinations revealed similarities but also considerable differences in the response signals. In principle, these differences may be attributed to either uncertainties in future social and economic development (here represented by the different emission scenarios) or to uncertainties in the formulation of the climate models including their internal variability.

For the long-term 99 percentile, the result of this analysis is shown in Fig. 10. For both extreme wind speeds and significant wave heights, the uncertainties introduced by different models are generally much larger than those caused by different scenarios. For wind speed the model-caused differences vary between about 0.2 and 0.8 m s^{-1}, which, for some areas, is larger than the overall mean climate change signal (Fig. 9). A similar conclusion holds for significant wave height where the model uncertainties range between about 0.1 and 0.6 m.

The model-caused differences increase from the southwest to the northeast, whereas the scenario-caused differences show a dipole pattern in which scenario A dominates (= positive changes) in the south and east and scenario B towards the north and west. The scenario-induced differences vary between about -0.2 and 0.15 m s^{-1} for extreme wind speeds and between about -0.2 and 0.1 m for extreme wave heights.

4 Discussion and Conclusions

The four emission/model combinations of future wave conditions show differences in both the amplitude and the spatial patterns of the climate change signals. In general, these differences can be attributed to respective differences in the climate change signals for future wind speed. The spatial difference patterns are relatively similar for the long-term 99 percentiles of the significant wave height and of the wind speed for a given emission/model combination. The largest uncertainties in the climate change signals occur in the northern part of the North Sea. For extreme significant wave heights, these uncertainties range up to 0.6-0.7 m south of the Norwegian coast. For extreme wind speeds, highest uncertainties are up to 0.9 m s^{-1} off the Danish coast. The smallest model-related uncertainties in the climate change signals of extreme wave height and wind speed are about 0.1 m and 0.2-0.4 m s^{-1}, respectively, and occur in the southwestern part of the model domain towards the English Channel.

One of the first attempts to quantify changes in extreme significant wave heights for the North Sea and the adjacent parts of the Northeast North Atlantic was provided by the WASA-Group (1998). They used regional output from a 6-year time slice experiment at about 75-km resolution for the expected time of CO_2 doubling to force a regional wave model with. Based on this rather short time series, they analyzed a moderate increase of the most severe significant wave heights in the North Sea. Using much longer time slice experiments, the STOWASUS-Group (2001) reached similar conclusions. Using output from a coupled climate model under three different greenhouse gas emission scenarios and by establishing statistical relationships between atmospheric sea level pressure fields and significant wave height, Wang et al. (2004)

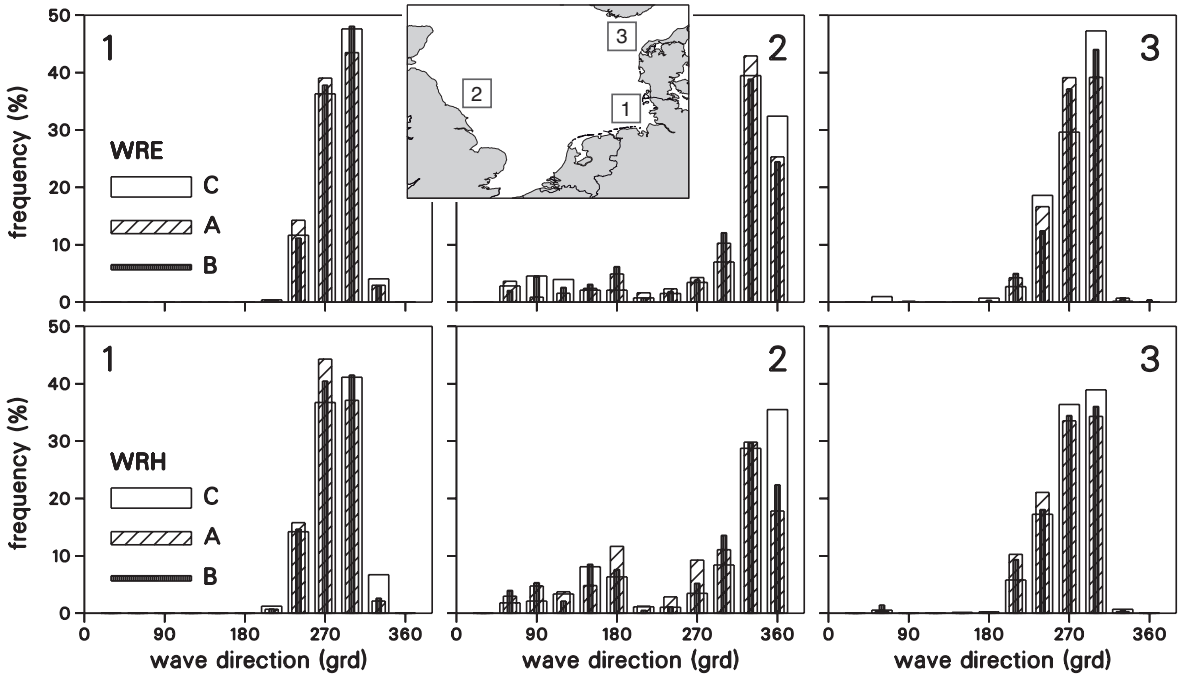

Fig. 8. Area averaged frequency distributions of wave directions for significant wave heights greater than the long-term 99 percentile for the three selected areas (see map inserted) for WRE (upper row) and WRH (lower row)

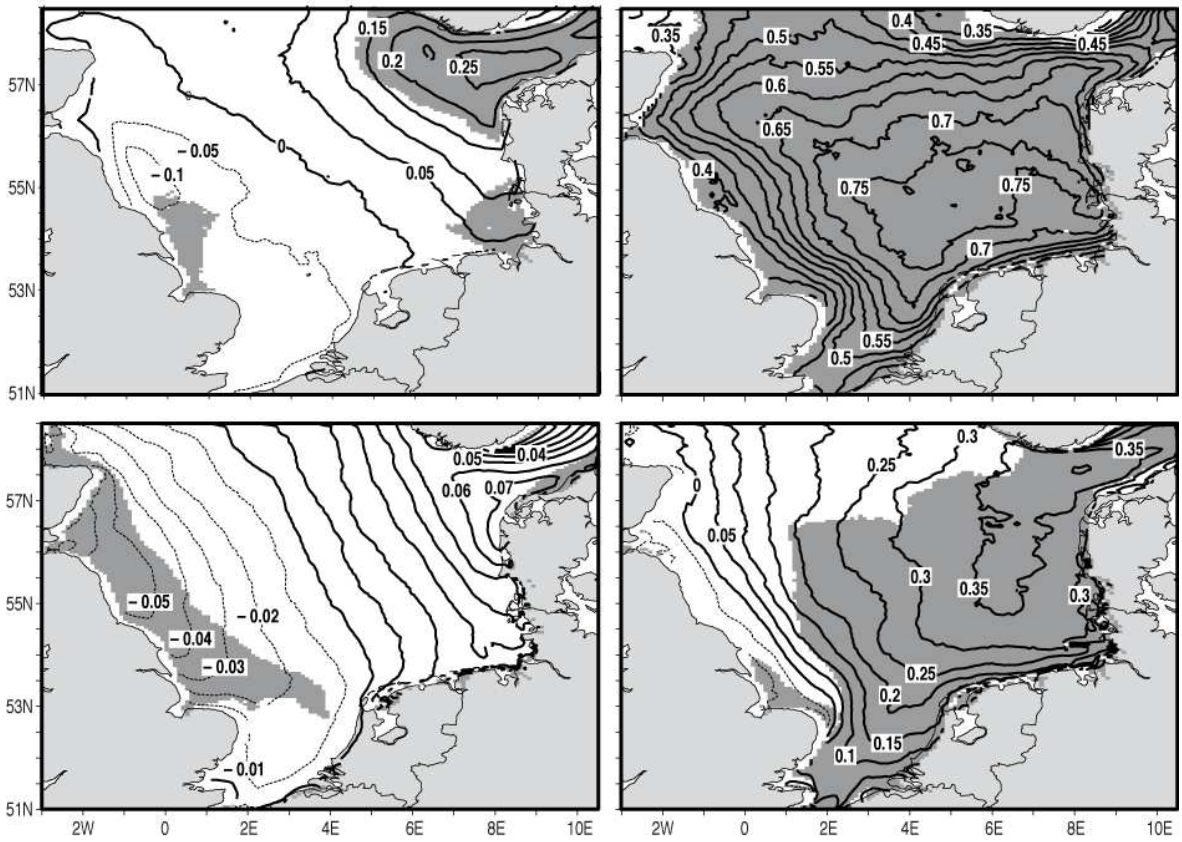

Fig. 9. Mean climate change signal $\overline{\Delta}$ for long-term 50 (left) and 99 percentile (right) wind speed in meters per second (upper row) and significant wave height in meters (lower row). Grey shading indicates areas where the climate change signal has at least the same sign in all simulations, i.e., for all scenarios and model realizations

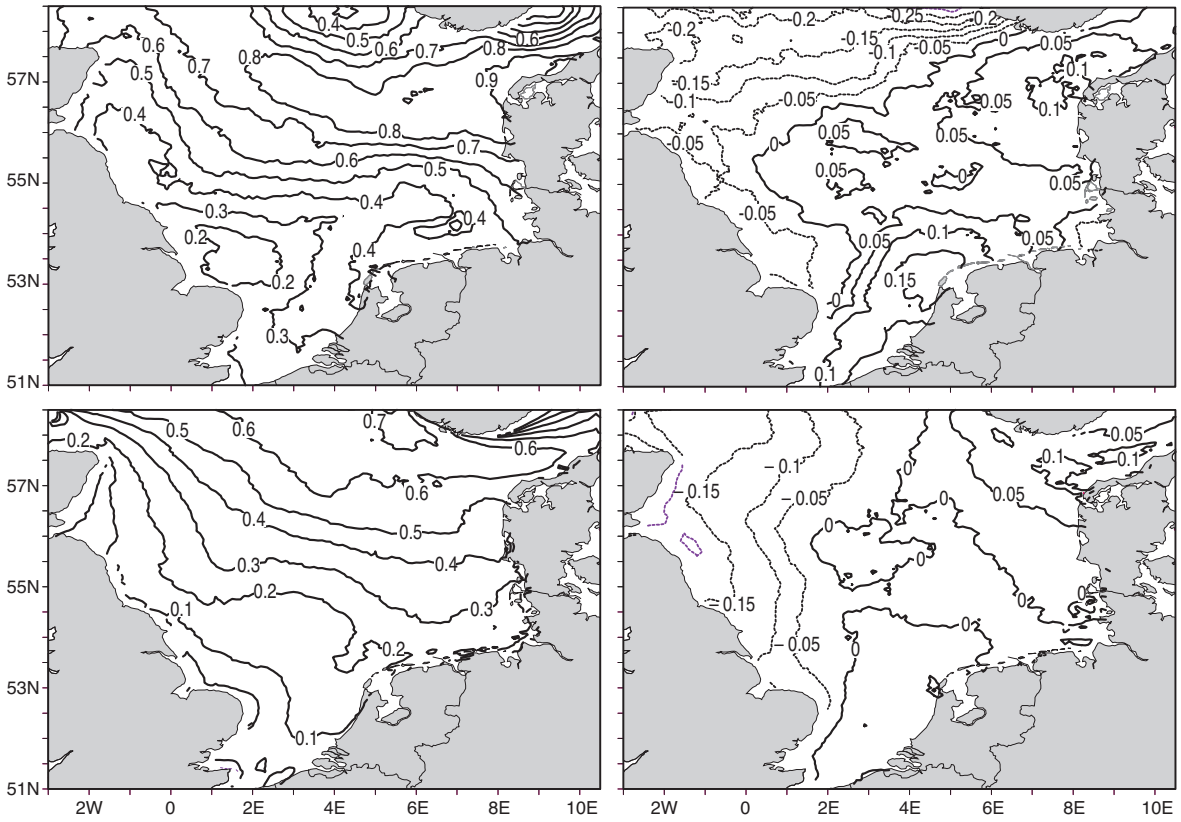

Fig. 10. Uncertainties caused by model differences $\Delta_{WRE,WRH}$ (left) and scenario choice $\Delta_{A,B}$ (right) for long-term 99 percentile wind speed in meters per second (upper row) and significant wave height in meters (lower row)

quantified uncertainties in the climate change signals for significant wave height caused by different economic developments. For the North Sea they report changes in extreme wave conditions whose rate and sign appear to be quite dependent on the forcing conditions. Using similar techniques but an ensemble of output from different climate change scenarios and models, Wang and Swail (2006) found that the uncertainty due to differences among the forcing scenarios is much smaller than that due to differences among the climate models.

The present study represents, to our knowledge, the first high-resolution, multimodel, and multiscenario ensemble study for severe wave conditions in the North Sea that is based on high-resolution, near-surface marine wind fields from a high-resolution regional climate model in combination with a dynamically forced wave model study. It therefore reduces the limitations of earlier studies, namely, the limited sample size and resolution. It complements the studies of Wang et al. (2004) and Wang and Swail (2006), which were based on a statistical approach and of global rather than of regional nature.

The results of this study are in principal agreement with those from earlier studies. In particular, we found a moderate increase of the most severe wave conditions in the North Sea towards the end of the century and a rather large uncertainty related to differences among the climate models. In accordance with the study of Wang and Swail (2006), we found those to be larger than those related to differences among the climate forcing-scenarios. In detail, the analysis of the four emission scenario/CGM combinations has shown that

1. There are large uncertainties in the magnitude and the spatial patterns of the climate change signals
2. The differences in future significant wave height between the different combinations are in the same order of magnitude as those between the control simulations for the two GCMs.

Whereas the scenario-induced differences show a dominance of scenario A2 in the southern and eastern parts of the North Sea and scenario B2 - by contrast - a dominance in the northern and western parts, the model-caused differences increase from the south (west) to the north (east). The model-caused differences are greater than the scenario-caused differences by a factor exceeding five in some regions. Thus, the influence of the "tool" GCM is larger than that of the different scenarios describing possible developments of society.

Despite the above mentioned uncertainties, there are, however, large areas where all models and all scenarios show at least the same sign for the future changes in extreme significant wave heights and wind speeds (Fig 9). From this, we conclude that, although statements about the amplitude of future wind and wave climate changes for the North Sea are associated with a high level of uncertainty, there may still be robust features in the climate change signals that may allow at least regional statements about the sign of the expected changes. There is agreement among the four climate realizations that extreme wave heights may increase by up to 0.35 m

(mean value for all combinations) in the Southern and Eastern North Sea for water depths exceeding 10 m towards the end of the twenty first century in case of global warming. A larger ensemble size is nevertheless required to consolidate this conclusion.

These findings give at least some ideas about the future behavior of wind and waves which can assist in medium and long-term planning for coastal and off-shore activities. The presented control and scenario simulations for the North Sea are suitable for analyzing extreme value statistics seaward of about 10-m water depth, while towards the coasts, additional downscaling is required to adequately account for small-scale bathymetry changes and shallow-water effects (Gaslikova and Weisse 2006). In addition, there are other factors that should be considered when discussing future waves in the shallower near-shore areas. There, the wave development depends on water depth and a possible rise in mean sea level, as well as possible morphological changes, both of which should be taken into account. For example, future changes in winds, currents, and waves may cause changes in the bathymetry of near-shore areas like the Wadden Sea along the Dutch, German, and Danish coasts. A possible rise of the wadden areas with rising mean sea level (which is especially important with respect to coastal protection) is still in question and is expected to depend on the sediment supply and on the strength and speed of the sea level rise (e.g. Ferk 1995; Flemming and Bartholomä 1997; Hofstede 1999; CPSL 2001). Thus, if the combination of mean sea level rise and possible near-shore topographical changes would result in larger water depths over the wadden areas and in a decrease of the dike forelands, waves may become higher in the Wadden Sea and could run up closer to the coasts increasing - together with the mean sea level rise - the risk-of-failure of coastal defences. For a part of the inner German Bight, such changes are exemplarily discussed in Wittig et al. (2007).

Summarizing, it can be concluded that, despite the remaining uncertainties, extreme wind speeds and wave conditions are likely to show a moderate increase in the eastern part of the North Sea, including the German Bight, towards the end of this century in case of global warming. In this case, human activities in the German Bight and along its coastal strips may be confronted not only with higher waves but also with longer-lasting and more frequent wave induced impacts.

Acknowledgments: The atmospheric data used to drive the wave model with and the sea ice data used as boundary conditions in the coarse grid WAM simulations were kindly provided by the Swedish Meteorological and Hydrological Institute (SMHI, Rossby Centre). The bathymetry for the fine WAM grid was obtained from the Bundesanstalt für Wasserbau, Dienststelle Hamburg. The authors are thankful to Ms. Gardeike for assistance with the graphics.

References

Alexandersson H, Tuomenvirta H, Schmidth T, Iden K (2000) Trends of storms in NW Europe derived from an updated pressure data set. Clim Res 14: 71–73

CPSL (2001) Final Report of the Trilateral Working Group on Coastal Protection and Sea Level Rise, Wadden Sea Ecosystem No. 13, Common Wadden Sea Secretariat. Wilhelmshaven, Germany

Debernard J, Røed L (2008) Future wind, wave and storm surge climate in the Northern Seas: a revisit. Tellus 60: 427–438, doi: 10.1111/j.1600–0870.2008.00312.x

Debernard J, Sætra Ø, Røed L (2002) Future wind, wave and storm surge climate in the Northern Seas. Clim Res 23: 39–49

Ferk U (1995) Folgen eines beschleunigten Meeresspiegelanstiegs für die Wattgebiete der niedersächsischen Nordseeküste. Die Küste 57: 135–156

Feser F, Weisse R, von Storch H (2001) Multi-decadal atmospheric modeling for Europe yields multi-purpose data. Eos Trans 82: 305, 310

Flemming BW, Bartholomä A (1997) Response of the Wadden Sea to a rising sea level: a predictive empirical model. Deutsche Hydrogr Z 49: 343–353

Gaslikova L, Weisse R (2006) Estimating near-shore wave statistics from regional hindcasts using downscaling techniques. Ocean Dyn 56: 26–35, doi:10.1007/s10236–005–0041–2

Gordon C, Cooper C, Senior CA, Banks H, Gregory JM, Jones TC, Mitchell JFB, Wood RA (2000) The silumation of SST, sea ice extents and ocean heat transports in a version of the hadley centre coupled model without flux adjustments. Clim Dyn 16: 147–166

Günther H, Rosenthal W, Stawarz M, Carretero J, Gomez M, Lozano I, Serrano O, Reistad M (1998) The wave climate of the Northeast Atlantic over the period 1955-1994: The WASA wave hindcast. Global Atmos Ocean Syst 6: 121–164

Hofstede J (1999) Mögliche Auswirkungen eines Klimawandels im Wattenmeer. Petermanns Geogr Mitt 143: 305–314

Houghton J, Ding Y, Griggs D, Noguer M, van der Linden P, Dai X, Maskell K, Johnson C (eds.) (2001) Climate Change 2001: The scientific basis. Contribution of Working Group I to the Third Assessment Report of the Intergovernmental Panel on Climate Change, Cambridge University Press, New York

Jones C, Ullerstig A, Willén U, Hansson U (2004) The Rossby Centre regional atmospheric climate model (RCA). Part I: model climatology and performance characteristics for present climate over Europe. Ambio 33: 199–210

Nakicenovic N, Swart R (eds.) (2000) Special Report of the Intergovernmental Panel on Climate Change on Emission Scenarios Cambridge University Press, Cambridge, Summary available online at http://www.ipcc.ch/pub/reports.htm

Niemeyer HD, Kaiser R (1999) Seegang. in: Nationalparkverwaltung Niedersächsisches Wattenmeer & Umweltbundesamt (ed.) Umweltatlas Wattenmeer - Band 2 Ulmer, pp 28–29

Pryor S, Schoof J, Barthelmie R (2006) Winds of change? Projections of near-surface winds under climate change scenarios. Geophys Res Lett 33: L11702, doi:10.1029/2006/GL026000

Räisänen J, Hansson U, Ullerstig A, Döscher R, Graham L, Jones C, Meier H, Samuelsson P, Willén U (2004) European climate in the late twenty-first century: regional simulations with two driving global models and two forcing scenarios. Clim Dyn 22: 13–31, doi:10.1007/s00382–003–0365–x

Räisänen J, Hansson U, Ullerstig A, Döscher R, Graham LP, Jones C, Meier M, Samuelsson P, Willén U (2003) GCM driven simulations of recent and future climate with the Rossby Centre coupled atmosphere - Baltic Sea regional climate model RCAO. SMHI Reports Meteorology and Climatology 101. Available from SMHI, S-60176 Norrköpingm Sweden 61pp

Roeckner E, Bengtsson L, Feichter J, Lelieveld, Rodhe H (1999) Transient climate change simulations with a coupled atmosphere-ocean GCM including the trophospheric sulfur cycle. J Climate 12: 3004–3032

Rummukainen M, Räisäsen J, Bringfelt B, Ullerstig A, Omstedt A, Willén U, Hansson U, Jones C (2001) A regional climate model for northern europe: model description and results from the downscaling of two GCM control simulations. Clim Dyn 17: 339–359

STOWASUS-Group (2001) Synthesis of the STOWASUS-2100 project: regional storm, wave and surge scenarios

for the 2100 century, Report 01-3. Danish Climate Centre. http://www.dmi.dk/pub/STOWASUS-2100
WAMDI-Group (1988) The WAM model - a third generation ocean wave prediction model. J Phys Oceanogr 18: 1776–1810
Wang X, Swail V (2004) Historical and possible future changes of wave heights in northern hemisphere oceans. in: Perrie W (ed.) Atmosphere ocean interactions, vol 2. Wessex Institute of Technology Press, Ashurst
Wang X, Swail V (2006) Climate change signal and uncertainty in projections of ocean wave heights. Clim Dyn 26: 109–126, doi:10.1007/s00382–005–0080–x
Wang X, Zwiers F, Swail V (2004) North Atlantic ocean wave climate change scenarios for the twenthy-first century. J Climate 17: 2368–2383
WASA-Group (1998) Changing waves and storms in the Northeast Atlantic? Bull Am Meteorol Soc 79: 741–760
Weisse R, Feser F (2003) Evaluation of a method to reduce uncertainty in wind hindcasts performed with regional atmosphere models. Coast Eng 48: 211–225
Weisse R, Günther H (2007) Wave climate and long-term changes for the Southern North Sea obtained from high-resolution hindcast 1958-2002. Ocean Dyn 57: 161–172, doi: 10.1007/s10236–006–0094–x
Weisse R, von Storch H, Feser F (2005) Northeast Atlantic and North Sea storminess as simulated by a regional climate model 1958-2001 and comparison with observations. J Climate 18: 465–479, doi: 10.1175/JCLI–3281.1
Wittig S, Elsner A, Elsner W, Eppel DP, Grabemann I, Grabemann HJ, Kraft D, Mai S, Meyer V, Otte C, Schirmer M, Schuchardt B, Zimmermann C (2007) Der beschleunigte Meeresspiegelanstieg und die Küstenschutzsysteme: Ergebnisse der erweiterten Risikoanalyse. in: Schuchardt B, Schirmer M (eds.) Land unter? Klimawandel, Küstenschutz und Risikomanagement in Nordwestdeutschland: die Perspektive 2050, Oekom Verlag pp 93–113
Woth K (2005) North Sea storm surge statistics based on projections in a warmer climate: How important are the driving GCM and the chosen emission scenario? Geophys Res Lett 32: L22708, doi:10.1029/2005GL023762
Woth K, Weisse R, von Storch H (2006) Climate change and North Sea storm surge extremes: An ensemble study of storm surge extremes expected in a changed climate projected by four different regional climate models. Ocean Dyn 56: 3–15, doi:10.1007/s10236–005–0024–3